Solid−Liquid Phase Equilibria of *N*-Methylephedrine Enantiomers in Two Chiral Solvents

Henning Kaemmerer,*,† Samuel Kofi Tulashie,† Heike Lorenz,‡ and Andreas Seidel-Morgenstern†,‡

Otto von Guericke University, D-39106 Magdeburg, Germany, and Max Planck Institute for Dynamics of Complex Technical Systems, D-39106 Magdeburg, Germany

The ternary solubility phase diagrams of the *N*-methylephedrine species in two chiral solvents, (*S*)-ethyl lactate and (2*R*,3*R*)-diethyl tartrate, have been studied. Solubility measurements were performed for enantiomeric compositions and temperatures ranging from 1:1 mixtures to the pure enantiomer and from (273 to 313) K. Predicted ideal solubility curves of the *N*-methylephedrine species in both solvents revealed deviations from experimental data. The nonrandom two-liquid model was applied to quantify and parametrize these nonidealities and nonideal heterochiral interactions among the enantiomers by means of corresponding activity coefficients. The solvent−solute interactions were interpreted as nonchiral specific, since no asymmetry in the chiral systems were found. The selection of an appropriate solvent for a crystallization-based enantioseparation based on the shape of solubility isotherms is discussed.

Introduction

The resolution of chiral compounds is of enormous interest for pharmaceutical, agricultural, and food industries. The need for efficient techniques for the production of enantiomerically pure compounds is largely due to the increasing high demand for single enantiomers.[1] Resolution of racemic mixtures can be realized using various methods such as kinetic resolution (chemical and/or enzymatic catalysis), diastereomeric salt formation, preparative chromatography, preferential crystallization, or enantioselective membranes (e.g., molecularly imprinted polymers). Direct enantioselective crystallization from solution is considered to be an appropriate approach for the separation of chiral systems, which exhibit suitable thermodynamic properties, that is, conglomerate-forming systems with favorable shapes of solubility isotherms. A crystallization-based approach using chiral solvents was considered recently.[2] Regarding feasibility and yields, any asymmetry in the typical mirror symmetric ternary phase diagrams of a pair of enantiomers in a solvent should result in further improvements.

Within this study we have chosen *N*-methylephedrine as a model compound. *N*-Methylephedrine belongs to the class of ephedrines, which are possible stimulant drugs for the central nervous system.[3] In recent times, there has been an increasing interest in drugs that include ephedrine alkaloids because these compounds are known to have a weak amphetamine-like effect on the central nervous system (energy booster) and enhance calorie-burning activity when taken together with aspirin and caffeine. It is also commonly used as decongestant (to relieve nasal congestion) and against hypotension (low blood pressure).[4] Moreover, *N*-methylephedrine is extensively applied as a chiral resolving precursor to chiral supporting electrolytes, a catalyst for phase transfer, and a reducing agent.[5]

* Corresponding author. Address: Otto von Guericke University, Institute of Process Engineering, Mailbox 4120, D-39106 Magdeburg, Germany. Phone: +49 (0) 391 6110 281. Fax: +49 (0) 391 6110 593. E-mail: kaemmerer@mpi-magdeburg.mpg.de.
† Otto von Guericke University.
‡ Max Planck Institute for Dynamics of Complex Technical Systems.

A few solubility measurements on chiral substances in chiral solvents do exist in literature, for which unfortunately no phase diagrams are available and no statement regarding the shape of solubility isotherms is provided.[6−10] Bosnich and Watts[9] and Mizumachi[10] reported that the solubilities of the pair of enantiomers of *cis*-$[Co(en)_2Cl_2]ClO_4$ in (−)-2,3-butanediol and tri-α-diimine ruthenium(II) complexes, respectively, were different. This is considered as a highly favorable property.

The current work is concerned with the determination and analysis of the solid−liquid phase equilibrium (SLE) of *N*-methylephedrine enantiomers in the two chiral solvents, (*S*)-(−)-ethyl lactate and (2*R*,3*R*)-(+)-diethyl tartrate, in a wider temperature range. The aims of the study are two-fold. First, a determination of the corresponding SLE was performed to gain an insight in the shapes of the solubility ternary phase diagram. Second, we intend to evaluate whether differences in the thermodynamic properties with respect to chirality can be found for the systems considered. Predicted ideal solubilities of *N*-methylephedrine were compared with the obtained experimental data. The nonrandom two-liquid model (NRTL) was employed to correlate the determined experimental data introducing corresponding activity coefficients. The ternary solubility diagrams of the *N*-methylephedrine enantiomers in the chiral solvents were predicted on the basis of the model parameters determined from measured binary SLE and were compared to measured ternary solubility data.

Experimental Section

Materials. (1*S*, 2*R*)-(+)-*N*-methylephedrine ((1), Figure 1a) and (1*R*,2*S*)-(−)-*N*-methylephedrine ((2), Figure 1b) were purchased from Sigma-Aldrich with purities of ≥ 99 %.

As solvents, (*S*)-(−)-ethyl lactate ((3), Figure 2a) and (2*R*,3*R*)-(+)-diethyl tartrate ((4), Figure 2b), obtained from Fluka/Sigma-Aldrich Chemical Co., with purities of ≥ 99 % (GC sum of enantiomers), were used. For HPLC analysis 2-propanol from Merck KGaA, Darmstadt, with a purity of ≥ 99.5 % was applied.

10.1021/je900572c CCC: $40.75
Published on Web 10/16/2009

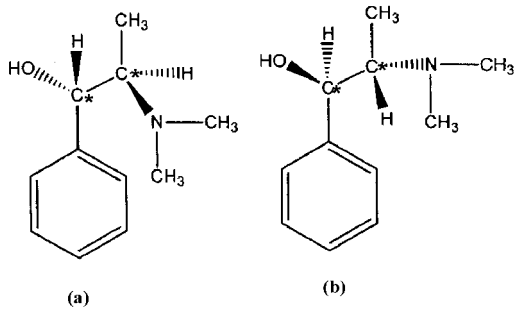

Figure 1. Chemical structures of the solute: (a) (1*S*,2*R*)-(+)-*N*-methylephedrine, (b) (1*R*,2*S*)-(−)-*N*-methylephedrine and with (*) representing the chiral center(s).

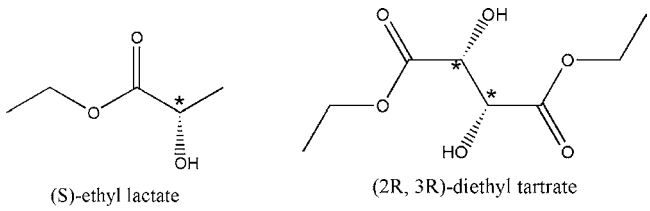

Figure 2. Chemical structures of the two solvents ((*S*)-ethyl lactate and (2*R*,3*R*)-diethyl tartrate) and with (*) representing the chiral center(s).

Apparatus and Procedure. The melting point and the enthalpy of fusion of *N*-methylephedrine were determined from analyses of DSC melting curves. Crystalline samples were crushed in a mortar and investigated using a DSC device (DSC 131, SETARAM, France; closed aluminum crucibles with approximately 12 mg of substance, a heating rate of 2 K·min^{-1}, and 8 mL·min^{-1} helium purge gas flow).

Dissolution kinetics experiments were performed for a racemic mixture of *N*-methylephedrine enantiomers and (1*S*,2*R*)-(+)-*N*-methylephedrine both in (*S*)-(−)-ethyl lactate and in (2*R*,3*R*)-(+)-diethyl tartrate at 278 K to evaluate the minimum time required to establish thermodynamic equilibrium. Liquid-phase samples were taken at specific time intervals from the suspension, and the concentrations were analyzed by high-performance liquid chromatography (HPLC). Equilibrium for both solvents was reached after approximately (8 and 6) h for a racemic *N*-methylephedrine mixture and (1*S*,2*R*)-(+)-*N*-methylephedrine, respectively. Accordingly, the experimental time was set sufficiently above these values to at least 24 h.

A classical isothermal method was applied for the determination of solubility isotherms for temperatures in the ranges of (273 to 298) K in (*S*)-(−)-ethyl lactate and of (298 to 313) K in (2*R*,3*R*)-(+)-diethyl tartrate, respectively. Hereby, a slurry consisting of 5 mL of solvent and a significant excess of solid phase was agitated by a magnetic stirrer and kept at isothermal conditions until equilibrium. Subsequently, the liquid and solid phases were separated using a glass filter (pore size, 10 μm) and analyzed separately. The liquid phase concentrations and the enantiomeric excess were determined by means of HPLC after dilution with 2-propanol (Agilent HP 1100; Eurocel OD column obtained through Knauer/Germany; 250 × 4.6 mm/5 μm; T = 298 K; UV: 254 nm; V_{eluent} = 1.0 mL·min^{-1}; eluent composition: φ (*n*-hexane) = 0.85, φ (2-propanol) = 0.15, φ (diethylamine) = 0.001). The solid phases of all samples were analyzed by X-ray powder diffraction (XRPD) to identify any crystalline modification (solvates and/or polymorphs) and to ensure that the same solid phase was always present. A PANalytical X'Pert Pro diffractometer (PANalytical GmbH, Germany) with Cu Kα radiation was used. The samples were prepared on Si sample holders, and the diffraction angle range was set to (3 to 40)° with a step size of 0.017° and a counting time of 50 s per step.

Reproducibility of the solubility measurements was studied in both solvents at the lowest and the highest temperatures considered by executing six experiments under the same conditions. Mole fraction solubility x_i as used for the equations in the following is defined as:

$$x_i = \frac{n_i}{\sum_{i=1}^{z} n_i} \tag{1}$$

with i being the constituents explained above and n_i the molar amount of the latter. The summation covers always the two enantiomers and either (*S*)-(−)-ethyl lactate or (2*R*,3*R*)-(+)-diethyl tartrate. In addition, mass fraction solubility w_i according to eq 2 is used in this paper, since this simplifies process design on the basis of graphical representations, for example, of ternary phase diagrams. Herein, m_i represents the mass of the constituent i.

$$w_i = \frac{m_i}{\sum_{i=1}^{z} m_i} \tag{2}$$

A first estimation of binary solubility was derived on the basis of the classical equation by Schröder and van Laar (eq 3).[11]

$$\ln(x_i^{\text{sat}}\gamma_i^{\text{l}}) = \frac{\Delta_{\text{fus}}H_i}{R}\left(\frac{1}{T_{\text{m,i}}} - \frac{1}{T}\right) \tag{3}$$

Hereby, the ideal solubility ($x^{\text{sat,id}}_i$) of a compound can readily be computed with the knowledge of the enthalpy of fusion and the melting temperature ($\Delta_{\text{fus}}H_i$, $T_{\text{m,i}}$) and by setting the liquid phase activity coefficient γ_i^{l} to unity in eq 3.

Results and Discussion

Calorimetric Properties and SLE. No additional or new phases (neither polymorphs nor solvates) differing from those of the pure enantiomers were identified from the results of the crystal lattice analysis by XRPD.

The enthalpy of fusion and the melting temperature of the *N*-methylephedrine enantiomers were determined as $T_{\text{m,i}}$ = 360.3 K and $\Delta_{\text{fus}}H_i$ = 29.24 kJ·mol^{-1} from repeated differential scanning calorimetry experiments (Table 1).

The obtained solubility data are summarized in Tables 2 and 3. The corresponding standard deviation analysis is given in Table 4. The experimentally determined solubilities of (1*R*,2*S*)-(−)-*N*-methylephedrine and (1*S*,2*R*)-(+)-*N*-methylephedrine in (*S*)-(−)-ethyl lactate or (2*R*,3*R*)-(+)-diethyl tartrate are presented as a function of temperature (symbols

Table 1. Error Analysis of the Measurement of Calorimetric Data of (1*S*,2*R*)-(+)-*N*-Methylephedrine (1)

number of experiments	$\Delta_{\text{fus}}H_i$ / kJ·mol^{-1}		$T_{\text{m,i}}$ / K	
n	mean	SD[a]	mean	SD[a]
5	29.24	0.42	360.3	0.02

[a] SD: standard deviation with n being the number of experiments, a_k the heat of fusion/melting point, and $\bar{a}$ the mean of all determined data points of the heat of fusion/the melting point. SD = $[1/(n-1)\sum_{k=1}^{n}(a_k - \bar{a})^2](1/2)$.

Table 2. Mass Fraction Solubility, w_i, of (1*S*,2*R*)-(+)-*N*-Methylephedrine (1) and (1*R*,2*S*)-(−)-*N*-Methylephedrine (2) in (*S*)-Ethyl Lactate (3) at Different Enantiomeric Excesses, ee [ee = $(w_1 - w_2)/(w_1 + w_2)$], in the Liquid Phase and for Different Temperatures

100 ee	100 $(w_1 + w_2)$	100 w_1	100 w_2	100 w_3
		$T = 273$ K		
100.00	11.68	11.68	0.00	88.32
40.00	17.19	12.03	5.16	82.81
0.00	21.96	10.98	10.98	78.04
40.00	17.09	5.13	11.96	82.91
100.00	11.10	0.00	11.10	88.90
		$T = 278$ K		
100.00	15.00	15.00	0.00	85.00
40.00	18.20	12.74	5.46	81.80
0.00	27.75	13.88	13.87	72.25
44.00	18.92	5.30	13.62	81.08
100.00	15.10	0.00	15.10	84.90
		$T = 288$ K		
100.00	18.73	18.73	0.00	81.27
50.00	23.31	17.48	5.83	76.69
0.00	34.50	17.25	17.25	65.50
40.00	23.31	6.99	16.32	76.69
100	19.26	0.00	19.26	80.74
		$T = 298$ K		
100.00	21.12	21.12	0.00	78.88
40.00	30.18	21.13	9.05	69.82
0.00	41.82	20.91	20.91	58.18
40.00	30.28	9.08	21.20	69.72
100.00	21.29	0.00	21.29	78.71

Table 3. Mass Fraction Solubility, w_i, of (1*S*,2*R*)-(+)-*N*-Methylephedrine (1) and (1*R*,2*S*)-(−)-*N*-Methylephedrine (2) in (2*R*,3*R*)-Diethyl Tartrate (4) at Different Enantiomeric Excesses, ee [ee = $(w_1 - w_2)/(w_1 + w_2)$], in the Liquid Phase and for Different Temperatures

100 ee	100 $(w_1 + w_2)$	100 w_1	100 w_2	100 w_4
		$T = 298$ K		
100.00	23.67	23.67	0.00	76.33
50.00	29.24	21.93	7.31	70.76
0.00	42.00	21.00	21.00	58.00
50.00	29.24	7.31	21.93	70.76
100.00	23.67	0.00	23.67	76.33
		$T = 303$ K		
100.00	28.00	28.00	00.00	72.00
40.00	33.00	23.10	9.90	67.00
0.00	46.50	23.25	23.25	53.50
40.00	33.00	9.90	23.10	67.00
100.00	29.00	29.00	0.00	71.00
		$T = 308$ K		
100.00	30.29	30.29	0.00	69.71
50.00	35.40	26.55	8.85	64.60
0.00	49.20	24.60	24.60	50.80
50.00	35.40	8.85	26.55	64.60
100	30.29	0.00	30.29	69.71
		$T = 313$ K		
100.00	36.28	36.28	0.00	63.72
30.00	44.75	29.09	15.66	55.25
0.00	55.58	27.79	27.79	44.42
50.00	40.99	10.25	30.74	59.01
100.00	35.63	0.00	35.63	64.37

in Figures 3 and 4). In addition, the predicted ideal solubilities (eq 3, $\gamma_i^l = 1$) in the two chiral solvents are shown by solid lines. The theoretical values and the determined solubilities increase with temperature in both solvents. They are approximately twice as high in (2*R*,3*R*)-(+)-diethyl tartrate in comparison to (*S*)-(−)-ethyl lactate. The experimental data in both solvents are clearly higher than the derived ideal solubilities of the *N*-methylephedrine enantiomers. Thus,

Table 4. Error Analysis of the Solubility Determination

T	(1*S*,2*R*)-(+)-*N*-methylephedrine (1) in (*S*)-(−)-ethyl lactate (3)		(1*S*,2*R*)-(+)-*N*-methylephedrine (1) in (2*R*,3*R*)-diethyl tartrate (4)	
K	n	SD[a] 100 w_i	n	SD[a] 100 w_i
273	6	0.04		
298	6	0.14	6	0.24
313			6	0.45

[a] SD: standard deviation with n being the number of experiments, w_k the solubility, and $\bar{w}$ the mean solubility. SD = $[1/(n-1)\sum_{k=1}^{n}(w_k - \bar{w})^2](1/2)$.

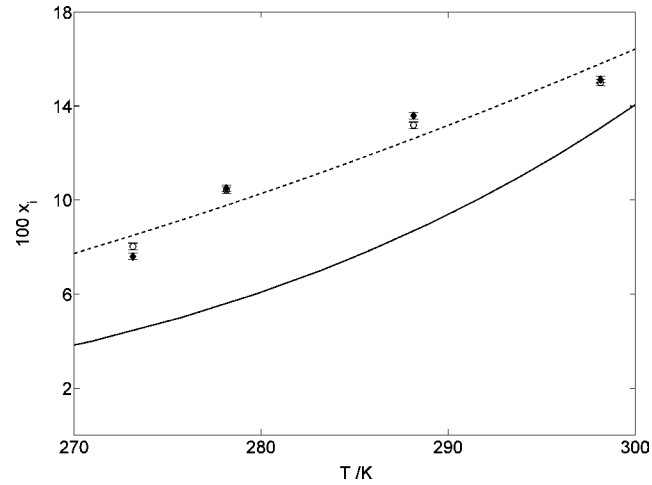

Figure 3. Mole fraction solubility of ○, (1*S*,2*R*)-(+)-*N*-methylephedrine (1) and ♦, (1*R*,2*S*)-(−)-*N*-methylephedrine (2) in (*S*)-ethyl lactate (3) between (273 and 298) K. Symbols are measurements, solid line: ideal solubility (eq 3, $\gamma_i^l = 1$), dashed line: NRTL model for (1*S*,2*R*)-(+)-*N*-methylephedrine (bold), error bars according to the derived maximal SD (Table 4).

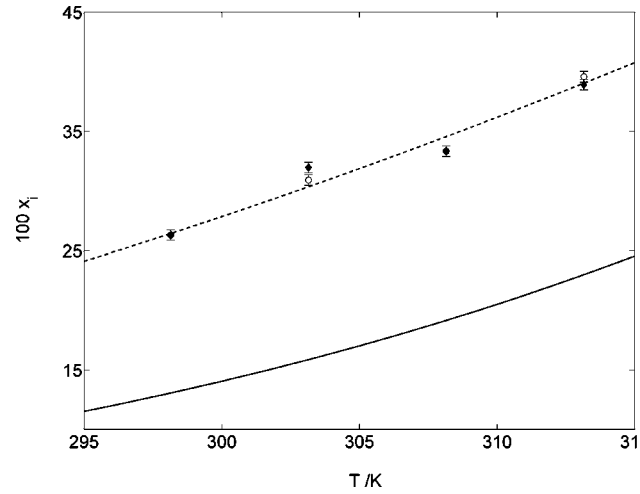

Figure 4. Mole fraction solubility of ○, (1*S*,2*R*)-(+)-*N*-methylephedrine (1) and ♦, (1*R*,2*S*)-(−)-*N*-methylephedrine (2) in (2*R*,3*R*)-diethyl tartrate (4) between (298 and 313) K. Symbols are measurements, solid line: ideal solubility (eq 3, $\gamma_i^l = 1$), dashed line: NRTL model for (1*S*,2*R*)-(+)-*N*-methylephedrine, error bars according to the derived maximal SD (Table 4).

significant attractive forces exist between (*S*)-(−)-ethyl lactate/(2*R*,3*R*)-(+)-diethyl tartrate and *N*-methylephedrine molecules.

Figures 5 and 6 illustrate the resulting ternary solubility phase diagrams of the *N*-methylephedrine enantiomers in (*S*)-(−)-ethyl lactate and (2*R*,3*R*)-(+)-diethyl tartrate. The diagrams show symmetrical mirror images with respect to the racemic axis,

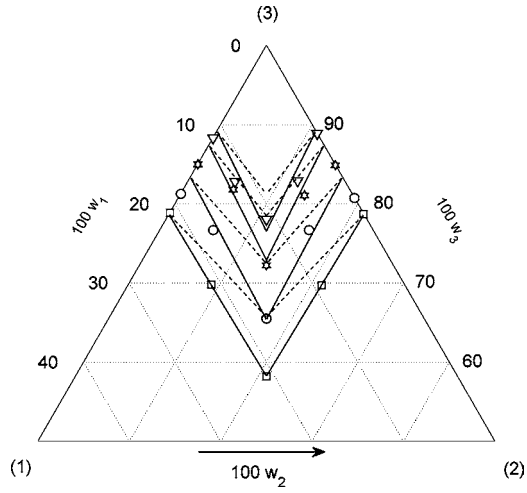

Figure 5. Mass fraction solubility isotherms of (1*S*,2*R*)-(+)-*N*-methylephedrine (1) and (1*R*,2*S*)-(−)-*N*-methylephedrine (2) in (*S*)-ethyl lactate (3) for: ▽, 273 K; ☆, 278 K; ○, 288 K; □, 298 K. Symbols represent experimental data, and lines are plotted according to the NRTL model (dashed: w/o heterochiral interactions, solid: with heterochiral interactions).

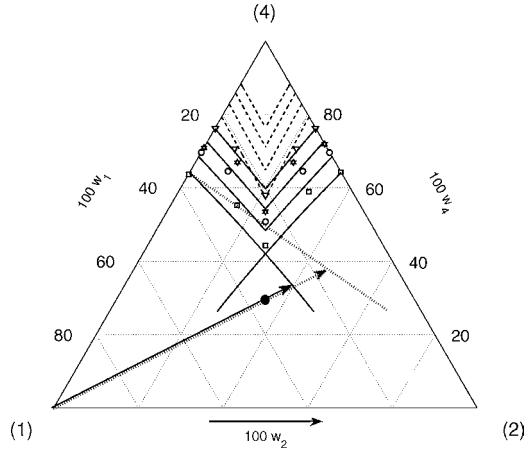

Figure 6. Mass fraction solubility isotherms of (1*S*,2*R*)-(+)-*N*-methylephedrine (1) and (1*R*,2*S*)-(−)-*N*-methylephedrine (2) in (2*R*,3*R*)-diethyl tartrate (4) for: ▽, 298 K; ☼, 303 K; ○, 308 K; □, 313 K. Symbols represent experimental data, and lines are plotted according to the NRTL model (solid) and for ideal solubilities with $\gamma_i^l = 1$ (dashed). The extended section of the solubility isotherm at 313 K represents the theoretical metastable continuation of the solubility isotherm on the basis of applied NRTL model. The dotted line stands for a fictive solubility isotherm in a system exhibiting a low α_{mol} value. The two arrows indicate the theoretical crystallization trajectories for the seeded crystallization processes of enantiomer 1 starting both with a supersaturated solution of 1:1 ratio of the enantiomers (full dot) and ending at the real metastable solubility isotherm (solid arrow) and the fictive metastable solubility isotherm (dotted arrow), respectively.

rather than asymmetry which is possible in chiral solvents. As known from the binary phase diagram of the chiral system, *N*-methylephedrine enantiomers do not form a racemic compound but rather a simple eutectic (conglomerate) system.[5] This was confirmed by the determined ternary phase diagrams. The general shape of both ternary systems is rather similar, while the solubility isotherms are clearly steeper in (*S*)-(−)-ethyl lactate than in (2*R*,3*R*)-(+)-diethyl tartrate.

This aspect is reflected in the so-called solubility ratio (α_{mol}). The α_{mol} value is defined as the ratio of the solubility of a racemic mixture of the enantiomers to that of a single enantiomer (both in mole fractions). It has been determined for (*S*)-(−)-ethyl lactate to be about 2 (1.95 at 273 K, 2.14 at 298 K) and for (2*R*,3*R*)-(+)-diethyl tartrate to be significantly smaller (1.73 at 298 K, 1.49 at 313 K), revealing a clear deviation from ideal behavior for this system. One has to be aware that this statement does hold only in one direction. An ideal system always exhibits α_{mol} values equal to 2 according to the "double solubility" rule by Meyerhoffer,[12] while also very nonideal systems like *N*-methylephedrine in (*S*)-(−)-ethyl lactate can have α_{mol} values close to 2. Such an α_{mol} value means that the solubility of one enantiomer is not (strongly) affected by the other one. Much smaller α_{mol} values account for a decrease in solubility of one enantiomer in the presence of the other enantiomer. Accordingly, at large α_{mol} values, the solubility of one enantiomer increases significantly by the presence of the other enantiomer. One example for the *N*-methylephedrine system in a nonchiral solvent is given by Wang et al. for a 2-propanol/water mixture.[5] Herein the α_{mol} value exhibits much larger values than 2.

It is known that the α_{mol} value has a large influence on the possible productivity of preferential crystallization strategies because of the change in the slope of the metastable solubility isotherms (the extended solubility isotherm was calculated using the NRTL model at $T = 313$ K in Figure 6). A comprehensive discussion of this aspect is reported by Collet and Jacques, Levilain et al., Collet et al., and Polenske et al.[11,13−15] In theory, the crystallization trajectories of a seeded preferential crystallization process are extended for small α_{mol} values, and more target enantiomer can be crystallized and harvested, provided that no nucleation of the undesired counter enantiomer takes place (Figure 6, enantiomer 2). The different lengths of the dotted arrow (pointing toward the fictive "flat" metastable solubility isotherm) and the solid arrow (pointing toward the solubility isotherm according to the NRTL model) in Figure 6 represent this aspect schematically. Considering the solubility ratios evaluated from the determined ternary solubility phase diagrams of *N*-methylephedrine, there is a rather wide area for entrainment; that is, it should be possible even to enter the outer two phase regions of the phase diagrams via crystallization (by crossing the phase boundary), which is more lucrative for obtaining enantiopure crystals. It is evident that no chiral solvent is required to alter the α_{mol} value to obtain favorable α_{mol} values.

Within this work an attempt is made to estimate α_{mol} values by a derivation of the ternary phase diagram on the basis of binary solubility data only. The dashed lines of Figure 6 have been drawn from the evaluation of the binary ideal solubilities and represent the slope of the ternary solubility isotherms for an ideal system of *N*-methylephedrine enantiomers in (2*R*,3*R*)-(+)-diethyl tartrate (i.e., $\gamma_i^l = 1$). Neither the absolute solubilities nor the shape of the phase diagram was captured correctly. Because of ideality, all α_{mol} values are exactly two, which results in larger deviations to the experimentally observed values mentioned above. Thus, a g^E model was parametrized to take into account nonidealities between the considered species.

g^E Model Parametrization and SLE Prediction. The multicomponent NRTL model (eq 4) was applied as done in previous papers, using the expressions for two components in the case of a single enantiomer in solution ($c = 2$) or three components in the case of a mixture of two enantiomers in solution ($c = 3$) (i,j: constituents).[16−18] Again, the summation covers always the two enantiomers and either (*S*)-(−)-ethyl lactate or (2*R*,3*R*)-(+)-diethyl tartrate.

$$\ln(\gamma_i^l) = \frac{\sum_{j=1}^{c} \tau_{ji} G_{ji} x_j}{\sum_{j=1}^{c} G_{ji} x_j} + \sum_{j=1}^{c} \frac{x_j G_{ij}}{\sum_{k=1}^{c} x_k G_{kj}} \left(\tau_{ij} - \frac{\sum_{k=1}^{c} x_k \tau_{kj} G_{kj}}{\sum_{k=1}^{c} x_k G_{kj}} \right) \quad (4)$$

First only solute−solvent interactions were considered, and heterochiral interactions among the enantiomers were neglected.[19−21] The three binary parameters $\alpha_{ji} = \alpha_{ij}$, g_{ji}, and g_{ij} were estimated by minimizing the objective function OF (eq 5) using the composition depending solution temperature at saturation of the predicted T^{calc} and the measured binary solubilities at T^{exp} of the *N*-methylephedrine enantiomers in each of the two solvents.

$$\mathrm{OF} = \min \sum_{k=1}^{N} \left(\frac{T_{k,i}^{exp}(x) - T_{k,i}^{calc}(\alpha_{ij}, g_{ij}, g_{ji}, x)}{T_{k,i}^{exp}(x)} \right)^2 \quad (5)$$

A Matlab (MathWorks, U.S.) routine using a Nelder-Mead optimizer was used. The parameter search was restricted to reasonable ranges. The temperature dependency of the activity coefficients was implemented in the NRTL model by the following expressions:

$$\tau_{ji} = \frac{g_{ji} - g_{ii}}{RT} \quad \tau_{ij} = \frac{g_{ij} - g_{ii}}{RT} \quad G_{ji} = \exp(-\alpha_{ji}\tau_{ji}) \quad G_{ij} = \exp(-\alpha_{ij}\tau_{ij}) \quad (6)$$

Third and higher-order interaction terms of the NRTL model were neglected, and the following assumptions were made because of the determined symmetry of the two considered systems: $\tau_{13} = \tau_{23}$, $\tau_{31} = \tau_{32}$, and $\alpha_{13} = \alpha_{23} = \alpha_{31} = \alpha_{32}$ (in the case of (*S*)-(−)-ethyl lactate (3)). This implies that the nonidealities among the solvent (3 or 4) and each enantiomer (1/2) were the same. The NRTL model was applied to account for the nonrandomness of these mixtures. The model (dashed thick lines in Figure 6) resemble the determined values quite closely over the whole temperature range in (2*R*,3*R*)-(+)-diethyl tartrate. The solubility in (*S*)-(−)-ethyl lactate was not well-captured. The obtained binary model parameters and the remaining deviations are given in Table 5. The deviations from ideality in both chiral solvents are exemplified in Figures 7 and 8 by means of plotting the theoretical activity coefficients of *N*-methylephedrine enantiomers as a function of temperature and composition. In addition, the activity coefficients have been plotted according to the NRTL model exemplarily for several solution compositions, which are under- or supersaturated and which do not only represent the solubility isotherm. The activity coefficients relevant for the determined solubility isotherms can be found on the solid bold lines and correspond to the values of Figures 3 and 4.

Table 5. Binary NRTL Model Parameter for the Two Systems: (1*S*,2*R*)-(+)-*N*-Methylephedrine (1) + (*S*)-(−)-Ethyl Lactate (3)/ (2*R*,3*R*)-(+)-Diethyl Tartrate (4)[a]

solvent	(*S*)-ethyl lactate (3)	(2*R*,3*R*)-diethyl tartrate (4)
α_{1j}	$2.411 \cdot 10^{-1}$	$9.870 \cdot 10^{-1}$
g_{1j}	$2.163 \cdot 10^{1}$ kJ·mol^{-1}	$2.252 \cdot 10^{6}$ kJ·mol^{-1}
g_{j1}	$-3.656 \cdot 10^{3}$ kJ·mol^{-1}	$-2.059 \cdot 10^{3}$ kJ·mol^{-1} kJ·
binary model deviation	$4.268 \cdot 10^{-4}$ K	8.286 10^{-5} K
α_{12}	$1.140 \cdot 10^{-12}$	0
g_{12}	$1.399 \cdot 10^{9}$ kJ·mol^{-1}	1 kJ·mol^{-1}
g_{21}	$-1.399 \cdot 10^{9}$ kJ·mol^{-1}	1 kJ·mol^{-1}

[a] Deviation from binary experimental data is calculated according to eq 5. Additional binary parameters α_{12}, g_{12}, and g_{21} for the system (1)/(2)/(3) are given.

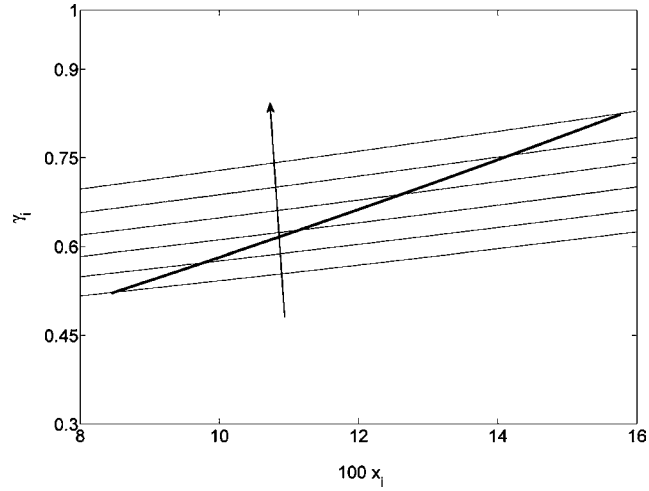

Figure 7. Temperature (arrow pointing toward higher values) and composition dependency of activity coefficients of (1*S*,2*R*)-(+)-*N*-methylephedrine in (*S*)-ethyl lactate according to the NRTL model for the given solution compositions and selected temperatures, (273, 278, 283, 288, 293, and 298) K. Activity coefficients of the saturated solution as used in Figure 1 are shown additionally (bold line).

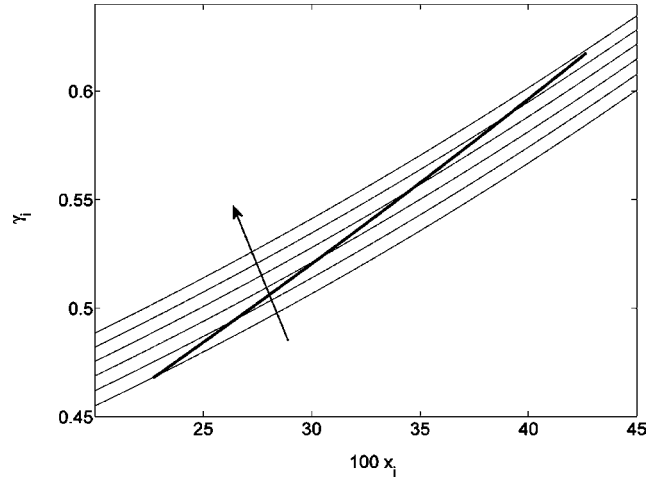

Figure 8. Temperature (arrow pointing toward higher values) and composition dependency of activity coefficients of (1*S*,2*R*)-(+)-*N*-methylephedrine in (2*R*,3*R*)-diethyl tartrate according to the NRTL model for the given solution compositions and selected temperatures, (293, 298, 303, 308, 313, and 318) K. Activity coefficients of the saturated solution as used in Figure 2 are shown additionally (bold line).

The accuracy of the prediction of the NRTL model is considered to be sufficient in the case of (2*R*,3*R*)-(+)-diethyl tartrate for further process design. The α_{mol} values were found as 1.65 at 298 K and 1.60 at 313 K, which is close to the experimentally determined values.

For the ternary phase diagram of *N*-methylephedrine enantiomers in (*S*)-(−)-ethyl lactate (dashed lines, Figure 5) larger deviations remained using the NRTL model, and the α_{mol} values were computed erroneously (1.76 at 273 K, 1.68 at 298 K). It is likely that the remaining deviations were due to pronounced heterochiral interactions among the enantiomers, which were not incorporated in the model but are known also from other systems of enantiomers.[19] For this reason a reparameterization was performed using the whole available data set. Hereby, the already derived binary parameters α_{13}, g_{13}, and g_{31} were kept constant, and additional model parameters α_{12}, g_{12}, and g_{21}

accounting for heterochiral interactions were fitted using eq 5 to ternary data. The resulting agreement to the measurement data was improved (solid lines, Figure 5), and the correct α_{mol} values were approached much closer (2.24 at 273 K, 2.1 at 298 K). Interestingly, heterochiral interactions are less prominent in the case of *N*-methylephedrine enantiomers in (2*R*,3*R*)-(+)-diethyl tartrate probably because of the more pronounced solvent−solute interactions. Both ternary phase diagrams have in common that the bent shapes of the solubility isotherms were not reflected by the predicted curves, which are almost linear. This is considered as a limitation of the NRTL model as applied here and makes a more accurate description necessary.

Conclusions

We investigated the solid−liquid phase equilibria of the conglomerate forming system *N*-methylephedrine in the two chiral solvents (*S*)-ethyl lactate and (2*R*,3*R*)-diethyl tartrate. A study of solubility data in the ternary systems was performed. No asymmetry was observed in the measured ternary solubility phase diagrams, while differences in the nonideal solubility behavior resulting in different shapes of the solubility isotherms were found.

The parametrization of the NRTL model with binary solubility data in (*S*)-(−)-ethyl lactate was possible with limited precision. Consequently, the predicted ternary phase diagram represented only partly the experimentally determined values. Therefore, interactions between the enantiomers were considered, and additional model parameters were introduced resulting in an improved agreement of experimental data and model prediction.

The activity coefficients are smaller for (2*R*,3*R*)-(+)-diethyl tartrate than for (*S*)-(−)-ethyl lactate in general. In summary, the solid−liquid phase equilibria of *N*-methylephedrine enantiomers in (2*R*,3*R*)-(+)-diethyl tartrate were predicted quite accurately on the basis of the model parametrization using only binary solubility data. It is likely that interactions between *N*-methylephedrine enantiomers and the (2*R*,3*R*)-(+)-diethyl tartrate prevail over the interactions of the enantiomers, since the second ternary phase diagram reflected the obtained measurements much better. For both solvents the magnitude of the solubility ratio was estimated correctly, while the general shapes of the bent solubility isotherms were not reflected well by the NRTL model prediction. In summary, the use of the applied model did result in reasonable improvements compared to the predicted ideal solubilities and α_{mol} values, but care must be taken if pronounced interaction between the enantiomer can be expected. (2*R*,3*R*)-(+)-diethyl tartrate is considered to be the better solvent for a chiral separation of the considered pair of enantiomers due to lower α_{mol} values.

Acknowledgment

The authors thank V. Subbarayudu-Sistla, C. Malwade, A. Hayoun, J. Kaufmann, and L. Borchert at the Max Planck Institute in Magdeburg for their help in the experimental work.

Literature Cited

(1) Caner, H.; Groner, E.; Levy, L.; Agranat, I. Trends in the development of chiral drugs. *Drug Discovery Today* **2004**, *9*, 105–110.

(2) Tulashie, S. K.; Lorenz, H.; Hilfert, L.; Edelmann, F. T.; Seidel-Morgenstern, A. Potential of Chiral Solvents for Enantioselective Crystallization. 1. Evaluation of Thermodynamic Effects. *Cryst. Growth Des.* **2008**, *8*, 3408–3414.

(3) Herráez-Hernández, R.; Campíns-Falcó, P. Chiral separation of ephedrines by liquid chromatography using [beta]-cyclodextrins. *Anal. Chim. Acta* **2001**, *434*, 315–324.

(4) Wang, M.; Marriott, P. J.; Chan, W.-H.; Lee, A. W. M.; Huie, C. W. Enantiomeric separation and quantification of ephedrine-type alkaloids in herbal materials by comprehensive two-dimensional gas chromatography. *J. Chromatogr., A* **2006**, *1112*, 361–368.

(5) Wang, X. J.; Wiehler, H.; Ching, C. B. Physicochemical Properties and the Crystallization Thermodynamics of the Pure Enantiomer and the Racemate for N-Methylephedrine. *J. Chem. Eng. Data* **2003**, *48*, 1092–1098.

(6) Yamamoto, M.; Yamamoto, Y. Stereospecific solute -- solvent interaction between [Lambda]-(+)D or [Delta]-(−)D-Co(en)33+ and L-(+)D-diethyltartrate appeared in solubility and viscosity. *J. Inorg. Nucl. Chem. Lett.* **1975**, *11*, 833–836.

(7) Amaya, K. Statistical Thermodynamics of Solutions of Optically Active Substances II. Solubility of d- and l-Isomers in Optically Active Solvents. *Bull. Chem. Soc. Jpn.* **1961**, *34*, 1803–1806.

(8) Jones, H. O. The Solubility of Stereoisomerides in Optically Active Solvents. *Proc. Cambridge Philos. Soc.* **1907**, *14*, 27–29.

(9) Bosnich, B.; Watts, D. W. Energetics of dissymmetric interactions. Differential solubility of d- and l- and dl-cis-$[Co(en)_2Cl_2]ClO_4$ and the enantiomerization in (−)-2,3-butanediol. *J. Am. Chem. Soc.* **1968**, *90*, 6228–6230.

(10) Mizumachi, K. The Solubility of Optically Active Tris---diimine Ruthenium(II) Complexes in 1−2-Methyl-1-Butanol. *J. Coord. Chem.* **1973**, *3*, 191–192.

(11) Jacques, J.; Collet, A. *Enantiomers, Racemates, and Resolutions*, reissue 1994 ed.; Krieger Publishing Company: Malabar, FL, 1981.

(12) Meyerhoffer, W. Stereochemische Notizen. *Ber. Dtsch. Chem. Ges.* **1904**, *37*, 2604–2610.

(13) Levilain, G.; Tauvel, G.; Coquerel, G. In *How homogenous equilibria between solvated enantiomers can modify the stable and metastable heterogenous equilibria*, Proc. 13th BIWIC; Jansens, J. P., ter Horst, J. H., Jiang, S., Eds.; IOS Press: Delft, The Netherlands, 2006; pp 244−250.

(14) Collet, A.; Brienne, M. J.; Jacques, J. Optical resolution by direct crystallization of enantiomer mixtures. *Chem. Rev.* **1980**, *80*, 215–230.

(15) Polenske, D.; Lorenz, H.; Seidel-Morgenstern, A. Separation of Propranolol Hydrochloride Enantiomers by Preferential Crystallization: Thermodynamic Basis and Experimental Verification. *Cryst. Growth Des.* **2007**, *7*, 1628–1634.

(16) Worlitschek, J.; Bosco, M.; Huber, M.; Gramlich, V.; Mazzotti, M. Solid-Liquid Equilibrium of Tröger's Base Enantiomers in Ethanol: Experiments and Modelling. *Helv. Chim. Acta* **2004**, *87*, 279–291.

(17) Kaemmerer, H.; Polenske, D.; Lorenz, H.; Seidel-Morgenstern, A. In *Selection and application of chiral resolution strategies for compound forming systems on the basis of solubility isotherms*, Proc. 15th BIWIC; Lorenz, H., Kaemmerer, H., Eds.; Shaker: Magdeburg, Germany, 2008; pp 42−49.

(18) Renon, H.; Prausnitz, J. M. Local compositions in thermodynamic excess functions for liquid mixtures. *AIChE J.* **1968**, *14*, 135–144.

(19) Kaemmerer, H.; Lorenz, H.; Seidel-Morgenstern, A. *Theoretical and experimental determination of solid-liquid equilibria of chiral compound forming systems in solution*, Proc. 17th ISIC; Jansens, J. P., Ulrich, J., Eds.; European Federation of Chemical Engineering: Maastricht, The Netherlands, 2008; pp 479−486.

(20) Wang, Y. Eutectic Composition of a Chiral Mixture Containing a Racemic Compound. *Org. Process Res. Dev.* **2005**, 670–676.

(21) Chen, A. M.; Wang, Y.; Wenslow, R. M. Purification of Partially Resolved Enantiomeric Mixtures with the Guidance of Ternary Phase Diagram. *Org. Process Res. Dev.* **2008**, *12*, 271–281.

Received for review July 7, 2009. Accepted September 23, 2009.

JE900572C